

Optimizing drone-assisted victim localization and identification in mass-disaster management: a study on feasible flying patterns and technical specifications

Intan Nabina Azmi¹, Murizah Kassim^{1,2}, Yusnani Mohd Yusoff^{1,3}, Nooritawati Md Tahir^{1,2,4,5}

¹School of Electrical Engineering, College of Engineering, Universiti Teknologi MARA, Shah Alam, Malaysia

²Institute for Big Data Analytics and Artificial Intelligence, Universiti Teknologi MARA, Shah Alam, Malaysia

³Information Security and Trusted Infrastructure Laboratory, Universiti Teknologi MARA, Shah Alam, Malaysia

⁴Department of Cybersecurity, International Information Technology University, Almaty, Kazakhstan

⁵Applied College, Princess Nourah bint Abdulrahman University, Riyadh, Saudi Arabia

Article Info

Article history:

Received Nov 17, 2023

Revised Mar 29, 2024

Accepted Apr 2, 2024

Keywords:

Drone-assisted

Flying-pattern

Mass-disaster management

Search and rescue

Victim identification

ABSTRACT

The prompt emphasizes the importance of identifying victims in a disaster area within 48 hours and highlights the potential benefits of using drones in search and rescue missions. However, the use of drones is limited by factors such as battery life, processing speed, and communication range. To address these limitations, the paper presents a detailed research study on the most effective flying pattern for drones during search and rescue missions. The study utilized energy consumption and coverage area as performance metrics and collected precise images that could be analyzed by the forensic team. The research was conducted using OMNET++ and fieldwork at Pulau Sebang, Melaka, in collaboration with search and rescue agencies in Malaysia. The results suggest that the square flying pattern is the most effective, as it provides the highest coverage area with reasonable energy utilization. Both simulation and fieldwork results showed coverage of 100% and 97.96%, respectively, for this pattern. Additionally, the paper provides technical specifications for rescue teams to use when deploying drones during search and rescue missions.

This is an open access article under the [CC BY-SA](https://creativecommons.org/licenses/by-sa/4.0/) license.



Corresponding Author:

Yusnani Mohd Yusoff

Information Security and Trusted Infrastructure Laboratory, College of Engineering, Universiti Teknologi MARA

Jalan Ilmu 1/1, 40450 Shah Alam, Selangor, Malaysia

Email: yusna233@uitm.edu.my

1. INTRODUCTION

The timely identification of victims within 48 hours is crucial from a forensic perspective as it ensures the quality and freshness of the body for accurate analysis. After 48 hours, the decomposition process begins, making it more challenging to produce a high-quality report. The significance of identifying victims within this timeframe extends beyond the forensic aspect as it can reduce processing time and costs for the family and other parties, including insurance companies. To achieve timely victim identification in hard-to-reach areas, drones equipped with advanced technology are becoming an increasingly attractive option. However, drone technology has limitations, such as restricted battery life, processing power, and communication range. Despite these challenges, drones have shown promise in search and rescue missions, as discussed in the following paragraph.

Drones have become increasingly popular in search and rescue (SAR) operations in remote and disaster-prone areas, as evidenced by numerous studies [1]–[5]. The use of wireless multi-hop end devices

has also been demonstrated to be effective in post-disaster scenarios [6], facilitating more efficient search efforts in larger areas and expediting the overall process. As a result, researchers continue to investigate essential aspects of drone technology, such as wireless connectivity and flying hours [7]–[9]. For communication in post-disaster areas, a wireless network with a wide transmission range is preferable. Communication technologies such as 5G [10], ad hoc networks [11], LoRa networks [12]–[15], and wireless network technology [16] are among the options available for drone communication. One proposed solution to address the issue of wireless connectivity is wireless flying ad-hoc networks (FANETs). An ad hoc network without a bulky infrastructure or central router, presents an efficient solution for establishing instant networking in post-disaster areas. It is capable of facilitating video streaming from drones to the base station [17]–[19]. In addition, mobility models are critical to avoid collisions and other obstacles during the drone's flight path [20]. To date, five different flying patterns have been identified: random-based, time-based, path-based, group-based, and topology-based [21]. The importance of identifying victims within the 48 golden hours has already been established from both medical and forensic perspectives. Thus, the emergence of advanced drone technology with systematic coordinates and flying patterns can optimize search and rescue missions.

Previous studies on the utilization of drones in real-world scenarios lacked in-depth analysis of technical specifications, a crucial aspect that must be addressed to enhance their effectiveness in aiding rescue teams during search and rescue operations in remote and inaccessible areas. The key focus of this study lies in identifying essential technical specifications, including optimal flying altitude, energy-efficient flying patterns, and camera requirements [22], crucial for empowering forensic teams with effective drone utilization during missions. These insights will serve as foundational guidelines for enhancing surveillance efficiency, minimizing redundancy, and conserving energy resources. The study has been conducted in collaboration with Aerodyne Group, Institute of Pathology, Laboratory and Forensic Medicine (I-PPerForM), National Institute of Forensic Medicine (Institut Perubatan Forensik Negara (IPFN)), Malaysia Civil Defence Force (APM), Malaysian Armed Forces (ATM), Royal Malaysia Police (PDRM), Analisa Resources Sdn Bhd, Faculty of Business Management and Faculty of Accountancy, UiTM, Faculty of Business and Accountancy, Universiti Selangor (UNISEL) and Graduate School of Business, SEGI University Institute Forensic Negara. The results have been validated by an expert from Aerodyne Group through simulation and fieldwork. This study's outcomes make significant contributions to drone-assisted victim localization and identification in mass-disaster management from a forensic perspective. The following sections will discuss the research methodology and the results and discussion while the research literature that guided the study is discussed in [23].

2. RESEARCH METHOD

This section outlines the approach used to achieve the objective. Three models of DJI drones (Phantom 3 Standard, 4 Pro, and Matrice 300 RTK) specifications are used in this study. This section consists of two main components: simulation and fieldwork. The simulation tests consist of two stages, where the first stage involves only DJI Phantom 3 Standard and 4 Pro, while the second stage involves the DJI Matrice 300 RTK. However, in the following paragraphs, these components will be combined and presented in a few technical sections.

2.1. Drone's flying pattern

To achieve the objective, this study employed a two-pronged approach consisting of simulation and fieldwork. The simulation was conducted using OMNeT++ version 5.2.1 and Inet version 3.6.3. It involved testing three flying patterns (circular, zigzag, and square) at altitudes of 10, 20, and 30 meters. The latter altitude was determined based on fieldwork tests conducted by Salem and Zaman [24]. The study found that the optimal altitude for affordable commercial drones was below 30 meters. The area covered and energy consumption were then calculated, and network performance was evaluated based on throughput and end-to-end delay.

The project utilized three DJI commercial drones and cameras, namely the DJI Phantom 3 Standard (DJI P3S), DJI Phantom 4 Pro (DJI P4P), and DJI Matrice 300 RTK. The technical specifications of these drones are listed in Table 1. The Phantom 3 Standard and Phantom 4 Pro have flight times of approximately 25 and 30 minutes, respectively. On the other hand, the DJI Matrice 300 RTK boasts a flight time of 60 minutes, making it the most technically advanced drone in the study.

To determine the most effective flying pattern for covering the largest area, flight tests were conducted at three different altitudes, encompassing a total area of 1 km². Two sets of tests were performed, with each set comprising nine scenarios involving the deployment of a single drone. These first-stage tests only involve DJI Phantom 3 Standard and 4 Pro, while DJI Matrice 300 RTK specification will be used in

another set of simulations to compare with the fieldwork. Both types of drones were utilized in these tests, and the drones were flown at a speed of 15 m/s, with additional parameters listed in Table 2.

Table 1. Types of drones with field of view and flight time

Specifications	DJI Phantom 3 Standard	DJI Phantom 4 Pro	DJI Matrice 300 RTK
Camera	N/A	N/A	H20T
Field of view	94°	63.7°	65° (H), 50° (V)
Flight time	Approx. 25 min	Approx. 30 min	Approx. 60 min
Take-off weight	1.216 kg	1.388 kg	6.3 kg

Table 2. List of parameters that required for simulation

Parameters	Preliminary simulation details	Fieldwork details
Flying area	1 km ²	0.2 km ²
Flying time	< 3600 s	< 350 s
Number of drones	1	1
Speed of drones	15 m/s	5 m/s
Flight altitude	10 m, 20 m, 30 m	40 m

2.2. Field of view angle

Figure 1 illustrates the drone's altitude and the camera's viewing range. The camera is assumed to be facing downwards to capture the maximum coverage area. The width of the field of view is influenced by the field of view angle's size and the distance between the lens and the ground. To calculate the drone's height (h) during flight, the field of view angle should be divided by 2. Equation (1) calculate the field of view, and subsequently, the value of y and the overall width of the field of view can be computed by multiplying it by 2.

$$y = (\tan \theta)(h) \quad (1)$$

where, y = The half side of field of view; and h = The drone's altitude in meter.

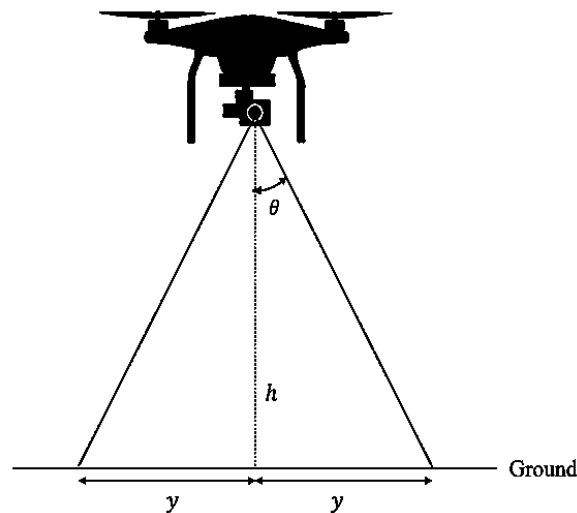


Figure 1. An Illustration of The FOV of drone's camera from above

2.3. Video transmission

Table 3 presents information regarding the video transmission capabilities of the three drones. The first drone has a bit rate of 40 Mbps and uses frequency ranges between 5.725 and 5.825 GHz for transmitting over a distance of 1 km. In comparison, the second drone offers a higher bit rate of 100 Mbps and can transmit over a longer range of 7 km. However, the technical specifications for the DJI Matrice 300 RTK used in the fieldwork is not available.

Table 3. Technical details of video transmission of each drone

Drone models	Bitrate	Operating frequency	Maximum distance
DJI Phantom 3 Standard	40 Mbps	5.725 - 5.825 GHz	±1 km
DJI Phantom 4 Pro	100 Mbps	2.400 - 2.483 GHz	±7 km
		5.725 - 5.825 GHz	
DJI Matrice 300 RTK	N/A	2.4000 - 2.4835 GHz	± 15 km
		5.725 - 5.850 GHz	

2.4. Drone's flying path

Despite their similar appearance, the DJI Phantom 3 Standard and 4 Pro have different embedded components, including the camera and battery. Consequently, the flight path for each drone must be planned separately due to the distinct types of cameras with varying field of view sizes. Table 4 presents the details of the flight tests for each pattern using the DJI Phantom 3 Standard and 4 Pro, including altitude and distance. Findings on the total percentage of the coverage area for each test has been presented and is available in [25].

Based on the data presented in Table 4, it is evident that with each increase in flight altitude, there's a notable decrease in flying distance for each flying pattern, primarily due to the expanded field of view at higher altitudes. Moreover, the analysis reveals a consistent trend where the DJI 4P exhibits a greater flying distance compared to the DJI P3S. This pattern of output should remain consistent during fieldwork implementation.

Table 4. Details of flight test for each pattern using DJI P3S and DJI P4P

Flying patterns	Flying altitude (m)	Flying distance (km)	
		DJI P3S	DJI P4P
Circular	10	31.7749	39.2881
Circular	20	17.2481	21.2092
Circular	30	13.0697	14.0912
Zigzag	10	37.4517	48.0298
Zigzag	20	19.9731	23.0592
Zigzag	30	13.0522	16.0072
Square	10	39.375	49.98
Square	20	21.845	24.96
Square	30	14.86	17.855

2.5. Drone's energy consumption

For this study, the energy consumption was calculated using the mathematical equation from previous research [26]. Simulation testing for the DJI Phantom 3 Standard and Phantom 4 Pro were conducted at a horizontal speed of 15 m/s, which was chosen due to its common use in previous research. Formula (9) based on previous research [27] was used to calculate the energy consumption during the turning phase. The drone's take-off weight considering the force of gravity, was determined using (2), which requires knowledge of the drone and payload mass as well as the acceleration due to gravity. The total take-off weight includes the drone body, propellers, batteries, and camera. All formula used in the study are listed below.

$$F_W = (m_d + m_p) g \quad (2)$$

where, F_W = The take-off weight with the gravity force; m_d = The mass of drone; m_p = The mass of the payload; and g = The gravity acceleration.

$$F_{DV} = \frac{1}{2} \rho A_t C_d v_v^2; F_{DH} = \frac{1}{2} \rho A_f C_d v_h^2 \quad (3)$$

where, F_{DV} , F_{DH} = The drag force in vertical and horizontal directions; ρ = The air density; A_t , A_f = The cross-sectional areas in vertical and horizontal directions; C_d = The drag coefficient; and v_v , v_h = The constant speed for vertical and horizontal flight.

$$\begin{aligned} F_{T,v} &= F_W + F_{DV} \\ &= (m_d + m_p) g + \frac{1}{2} \rho A_t C_d v_v^2 \end{aligned} \quad (4)$$

where, $F_{T,v}$ = The thrust force when the drone flies vertically.

$$\begin{aligned}
 F_{T,h} &= \sqrt{F_W^2 + F_{DH}^2} \\
 &= \sqrt{\left((m_d + m_p)g\right)^2 + \left(\frac{1}{2}\rho A_f C_d v_h^2\right)^2}
 \end{aligned} \tag{5}$$

where, $F_{T,h}$ = The thrust force when the drone flies horizontally.

$$F_T = 2\rho A_p C_d v_i^2 \tag{6}$$

where, F_T = The basic thrust calculation; A_p = The disk area of the propellers; and v_i = The induced velocity.

$$P_T = F_T v_i \tag{7}$$

where, P_T = The power consumption.

$$E_T = P_T \tag{8}$$

where, E_T = The energy consumption; and t = The time taken for a drone to fly vertical and horizontal.

$$E_{turn} = P_{turn} \frac{\Delta\theta}{\omega_{turn}} \tag{9}$$

where, E_{turn} = The energy consumption when the drone turns to follow the flight path; P_{turn} = The power consumption of the turning (260 W); $\Delta\theta$ = The turning angle performed by the drone; and ω_{turn} = The angular speed for turning (2.07 rad/sec).

$$E_{Total} = E_T + E_{turn} \tag{10}$$

where, E_{Total} = The total energy consumption of drone deployment in Joules (J)

The parameters listed in Table 5 are essential for calculating the energy consumption. However, to obtain the induced velocity for (6), a reverse engineering approach was employed. In a study by Hwang *et al.* [28], the drag coefficient for a hexa-rotor with a take-off weight of 14 kg was found to be most suitable at a value of 0.96. Based on this finding, a drag coefficient of 0.1 was assumed for both DJI Phantom models in this study.

Table 5. Details of parameters needed to calculate the energy consumptions

Parameters	DJI Phantom 3 Standard	DJI Phantom 4 Pro	DJI Matrice 300 RTK
Take-off weight (kg)	1.216	1.388	6.3
Gravitational force (m/s)	9.81	9.81	9.81
Air density (kg/s)	1.225	1.225	1.225
Area disk of propeller (m ²)	0.0098	0.010029	1.031
Drag coefficient	0.1	0.1	0.1
Horizontal speed (m/s)	15	15	2.5
Vertical speed-up (m/s)	5	5	1
Vertical speed-down (m/s)	3	3	1
Drone frontal area (m ²)	0.0139	0.0139	0.0952
Battery capacity (mah)	4480	5870	5935
Voltage (V)	15.2	15.2	52.8

2.6. Fieldwork study on drone surveying

A field test of the three flying patterns was conducted at Pulau Sebang, Malacca to validate the simulation results. However, due to limited drone flying approvals obtained from the Civil Aviation Authority of Malaysia (CAAM), the flight area in fieldwork was limited to 0.02 km². The drone used a DJI Matrice 300 RTK. Additionally, the flight altitude in the fieldwork was increased to 40 m to adapt to the circumstances. The test area, depicted in Figure 2, spans approximately 0.02 km² and is primarily used for agriculture operations and frog farming, specifically for cultivating pineapples and bananas. The terrain comprises flats, hills, and bushes, but no trees taller than 15 meters are present in the area. This location was deemed suitable for the research objectives as drone communication experienced minimal interference, resulting in a strong signal strength for the study.



Figure 2. Selected area for fieldwork operation

The fieldwork testing followed the flight path described in the previous subsection, but the drone flew at a lower altitude of 40 meters can harm the team and the drone itself. Since the actual implementation had its constraints and different drones were used, the flying specifications differed from the first stage of simulation. Thus, another set of simulations is designed to match with the fieldwork parameters for data and result analysis. The number of waypoints required in both situations is presented in Table 6. The simulations had a higher number of waypoints to ensure a smooth circular path compared to the fieldwork testing. These waypoints represent the points at which the drone will make turns.

Table 6. Details of flight test for each pattern using DJI Matrice 300 RTK during fieldwork and simulation

Patterns	Flight distance (m)		Estimated flight time (s)		Number of waypoints	
	Fieldwork	Simulation	Fieldwork	Simulation	Fieldwork	Simulation
Circular	607	607	275	189.6	23	55
Zigzag	830	830.7	347	218	10	10
Square	729	728.2	308	176	10	10

Figure 3 illustrates the circular, zigzag and square flying patterns plotted on the DJI Matrice 300 RTK controller and OMNeT++ platform. The left image was captured during the fieldwork, while the right figure was generated using the OMNeT++ simulator, representing the same distance as the field test. These visuals offer comparative insights into the performance of different flight patterns under similar conditions.

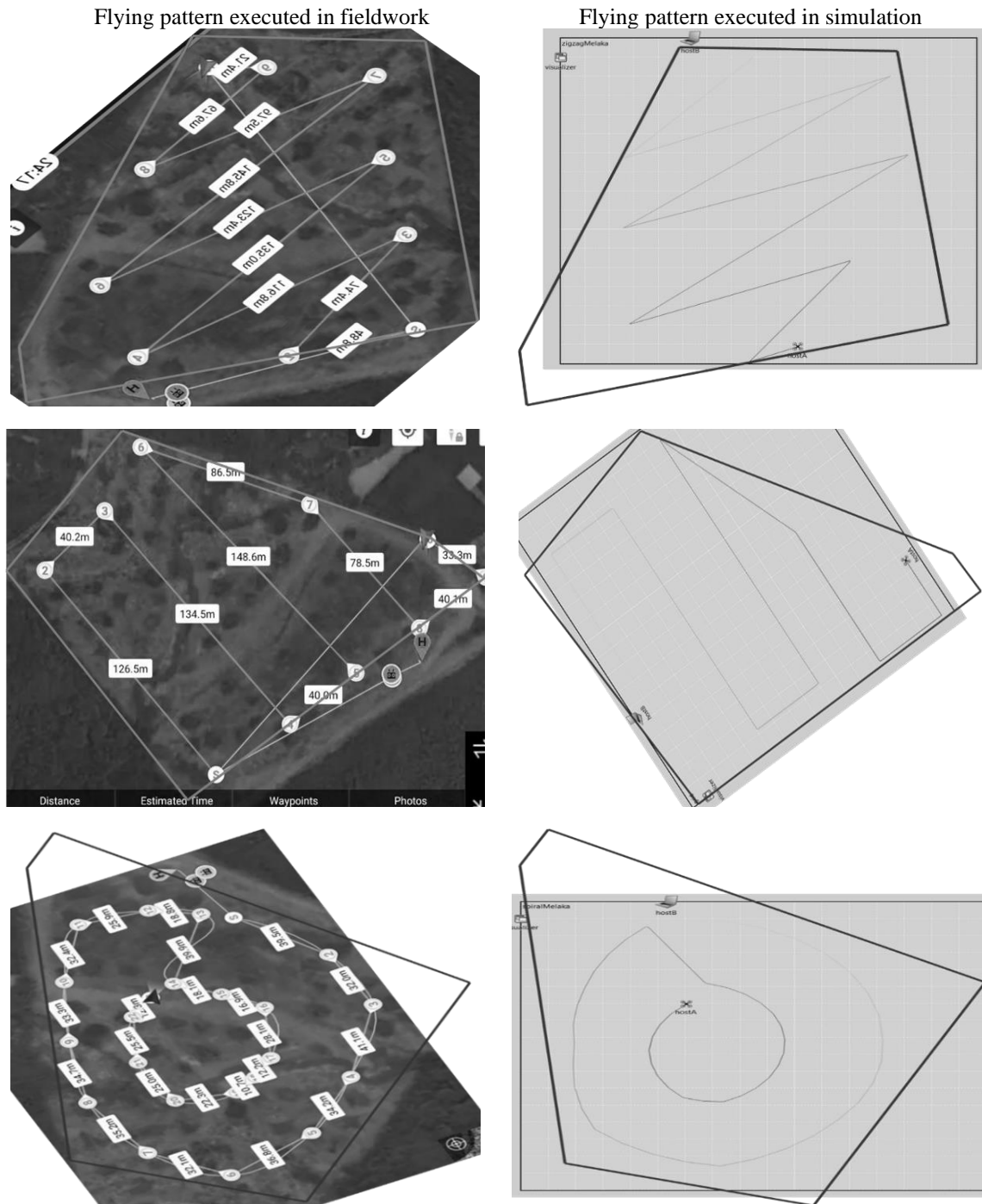


Figure 3. Flying pattern executed in fieldwork and simulation

3. RESULTS AND DISCUSSION

In this section, the findings based on the objectives are summarized. The first objective is to determine the most optimal flying pattern that results in the lowest energy consumption and the highest coverage area for victim identification within the 48-hour golden time period. The second objective is to compile a set of minimum technical specifications as a reference for forensic teams using drones during search and rescue missions.

3.1. Feasible flying pattern

Figure 4 shows the results from the simulation to determine the flying pattern with the lowest energy consumption. Referring to the graph in Figure 4, Phantom 3 Standard with the zigzag pattern consumed the

lowest energy than others with 512 kJ 30 meters height. This is followed by the square pattern with 579.9 kJ using the same type of drone. Besides, Phantom 4 Pro with circular and square patterns consumed the highest energy. The energy consumption is 875.6 kJ and 745.7 kJ, respectively. In all flying patterns, the energy decreased significantly from 10 to 20 meters in height.

It can be concluded that the zigzag flying pattern consumed the least energy. Furthermore, the square flying pattern, despite covering the largest area, also consumes a relatively low amount of energy at every altitude. These findings show potential energy savings for both flying patterns.

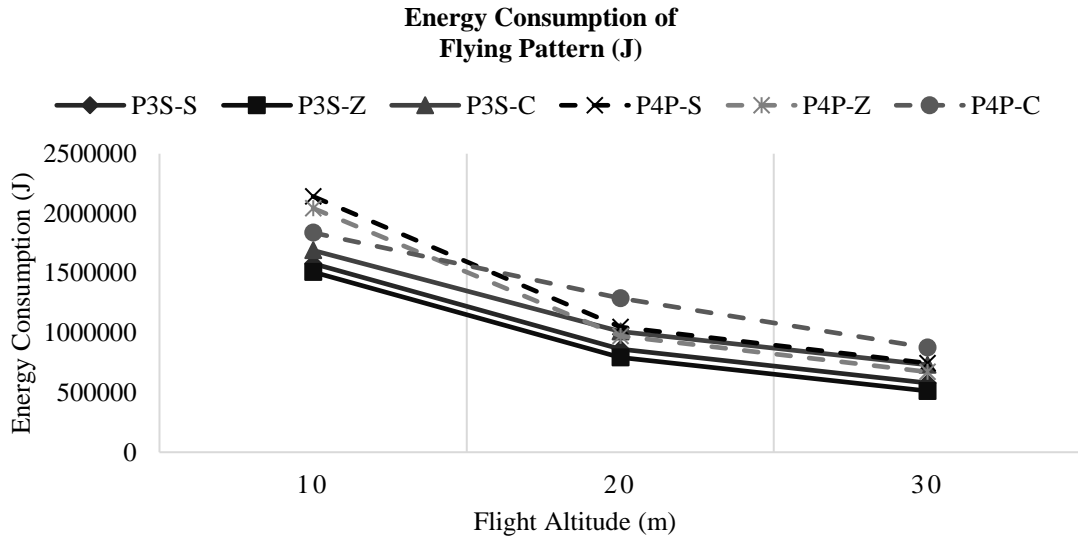


Figure 4. Energy consumption of flying patterns (J)

Referring to the graph in Figure 5, the x-axis starts with the value 0. The figure shows the data collected with a minimum value of 60. Furthermore, the straight line in the Figure 5 represents the Phantom 3 Standard drone, while the dotted line represents the Phantom 4 Pro drone. Phantom 3 Standard with a square flying pattern outperforms the others with the percentage of the covered area of 94.84% at 30 meters height. This is followed by Phantom 4 Pro with 93.87% using a similar flying pattern. The zigzag flying pattern, on the other hand, shows the lowest coverage area for both types of drones, with a coverage area of 66.84% and 69.80% for Phantom 3 Standard and Phantom 4 Pro, respectively.

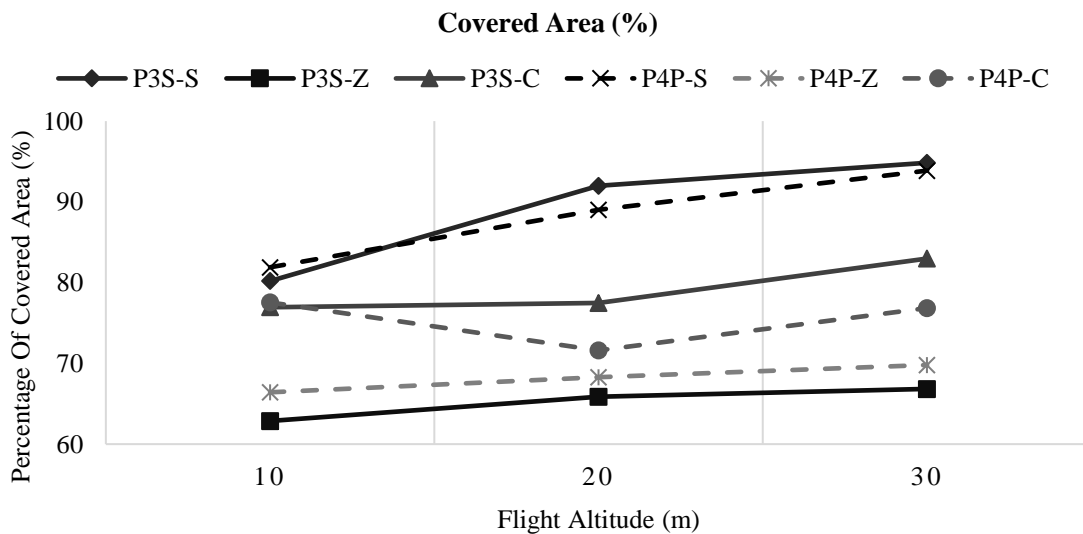


Figure 5. The percentage of covered area from 18 scenarios

For both types of drones depicted in Figure 5, it was observed that employing a square flying pattern provides the broadest coverage for surveillance purposes. Furthermore, the study revealed that specific drone specifications play a crucial role in augmenting the extent of surveillance coverage. Notably, an important discovery was made regarding the positive correlation between drone flying altitude and expanded surveillance area, suggesting that higher altitudes lead to improved coverage.

The energy consumption for the drone flying in three different flying patterns was calculated using the formulas in (2) to (10), and the results are shown in Figure 6. The percentage value refers to the battery percentage before flying and immediately after it returns to the base station. These results offer a comparative analysis of energy usage across various flight patterns, providing valuable insights for optimizing drone operations.

Figure 7 presents the results on the percentage of covered area for three different flying patterns in two different environments. In both environments, the square flying pattern shows the highest coverage of 100% during simulation and 97.96% in the fieldwork. These findings underscore the effectiveness of the square pattern in maximizing coverage across varying environmental conditions.

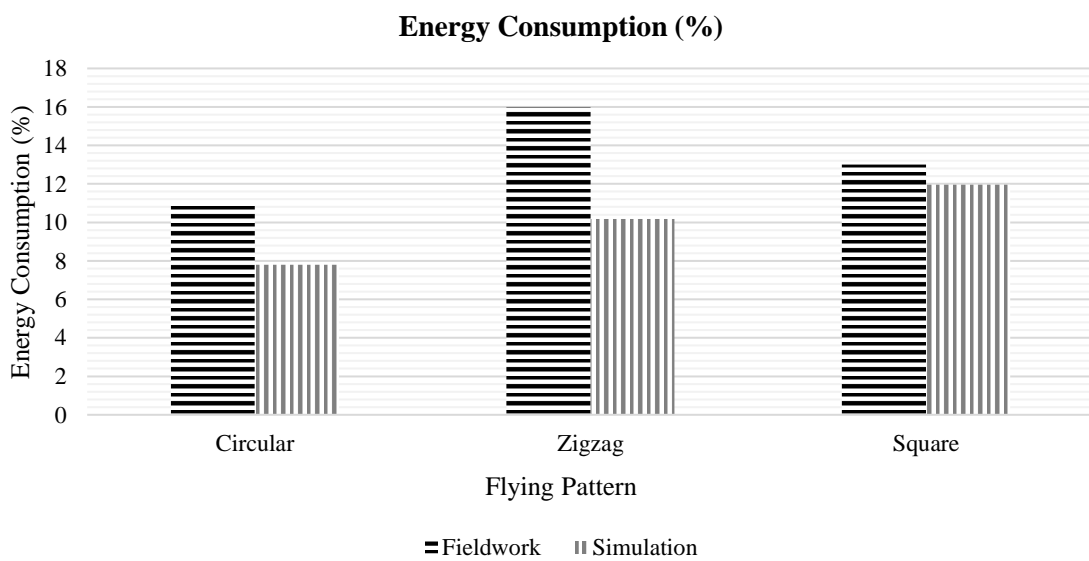


Figure 6. Energy consumption for drone flying

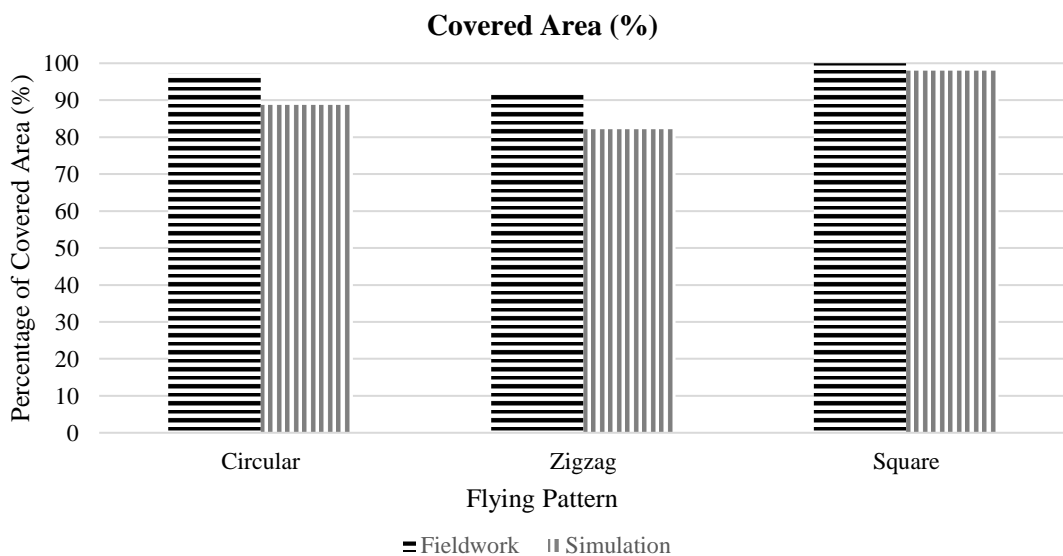


Figure 7. Percentage of covered area for 3 different flying patterns

Based on the results presented in Figures 6 and 7, the circular flying pattern consumes the lowest energy in both simulation and fieldwork conditions due to its shorter flying distance. However, the video footage captured from the circular pattern is not clear, especially on the left side of the images. On the other hand, the square flying pattern has the second-lowest energy consumption and provides clear video outcomes. Therefore, the square flying pattern is considered the best choice in terms of energy consumption and video quality for SAR missions. Additionally, the square pattern covers the smallest dark spot area, making it ideal for victim identification within the 48-hour golden time frame. Moreover, the square pattern has also been applied in other researches [29], [30], providing strong evidence that this path planning pattern is practical to apply in the real world. However, technical parameters such as the flying altitude with drone technical specifications (battery lifetime and camera) remain undiscussed. Thus, this study is conducted with three types of drone models to fill the gaps.

3.2. Minimum technical specification

This section presents the minimum technical specifications for drone implementation based on data collected from simulations and fieldwork. The key parameters for drone applications include camera features, altitudes, battery capacity, and communication range. Table 7 displays the data obtained from the square flying pattern. The DJI Phantom 3 Standard has a wider field of view angle compared to the DJI Phantom 4 Pro, but both cameras lack zooming features.

Table 7. Comparison of drone minimum technical specification

Parameters	DJI Phantom 3 Standard	DJI Phantom 4 Pro
Altitudes,	$h = 10$ m	$h = 10$ m
Field of View	$2y = 21.4$ m	$2y = 18$ m
	$h = 20$ m	$h = 20$ m
	$2y = 42.8$ m	$2y = 36$ m
	$h = 30$ m	$h = 30$ m
Battery Capacity Needed	$2y = 64.4$ m	$2y = 54$ m
	$h = 10$ m	$h = 10$ m
	BA = 1605800.3 J (7 batteries)	BA = 2163189.1 J (7 batteries)
	$h = 20$ m	$h = 20$ m
	BA = 888770.0 J (4 batteries)	BA = 1078377.2 J (4 batteries)
Communication Range	$h = 30$ m	$h = 30$ m
	BA = 607365.3 J (3 batteries)	BA = 768930.1 J (3 batteries)
	1 km	7 km

Furthermore, the energy required to complete the flight path at different altitudes indicates that both drones require the same number of batteries for each altitude. However, the DJI Phantom 4 Pro has a wider communication range than the DJI Phantom 3 Standard. The field of view width data can be used for drone implementation, where the obtained field of view width represents the optimal distance between two lines of the flight path. If the distance between the first and second paths is smaller than the value of $2y$, there is redundant information.

Table 8 outlines the minimum technical specifications for drone implementation to determine the optimal camera features and altitudes. Flying the drone at higher altitudes requires lower energy consumption due to the wider field of view, resulting in shorter flight distances to complete the flying pattern in the designated area. The DJI Matrice 300 RTK camera is equipped with zoom capabilities, making it suitable for deployment at higher altitudes and capturing clearer images.

Based on this observation, it can be inferred that actual drone implementation may encounter natural obstacles such as wind, which would require additional energy and time to maintain the drone's position and complete the flight path. It is also evident that the camera specifications play a crucial role in achieving better surveillance at a higher altitude of 30 meters while maintaining reasonable energy consumption. Finally, Table 9 summarizes the minimum technical specifications and requirements for using drones to assist in victim localization and identification during mass-disaster management.

Previous studies that employed drone path planning flying patterns have neglected to delve deeper into the specific requirements associated with drone operation. While the researchers did mention drone specifications and survey areas, there is a lack of analysis in medical and forensic aspects [29], [30]. The technical specifications acquired in this study can significantly enhance the efficiency of search and rescue missions for the rescue team.

Table 8. Comparison of technical specification in fieldwork vs simulation

Parameters	Fieldwork	Simulation
Altitudes,	$h = 40$ m	$h = 40$ m
Field of view	$y_h = 25.48$ m $y_v = 18.65$ m $2y_h = 50.96$ m	$y_h = 25.48$ m $y_v = 18.65$ m $2y_h = 50.96$ m
Battery capacity	$h = 40$ m BA = 293312.5 J (13% of 1 battery)	$h = 40$ m BA = 269914.6 J (12% of 1 battery)
Zoom features	20 MP	N/A
Testing time	310 s	176 s

Table 9. Minimum technical specifications and requirements in utilizing drone

Parameters	Small Drone	Big Drone
Camera	No zoom	With zoom
Field of view	$> 65^\circ$	$< 65^\circ$
Altitude (ASL)	20 m	40 m
Battery capacity	5870 mAh	5935 mAh x 2

4. CONCLUSION

In conclusion, following comprehensive simulations and field tests, the square flying pattern has been determined as the optimal choice for drones employed in search and rescue missions within post-disaster areas. This pattern ensures complete coverage while maintaining reasonable energy consumption. When coupled with the recommended minimum technical specifications, search and rescue teams are poised to capture clear footage of victims within the critical 48-hour window. The findings of this research hold significant implications for various agencies involved in search and rescue missions, including insurance companies and society as a whole. Implementing drones equipped with square flying patterns can expedite rescue efforts, facilitating the more efficient location and identification of victims, potentially saving lives. It is worth noting that drone missions are subject to weather conditions and may be impacted by strong winds and heavy rain. This aspect presents a promising area for future research aimed at developing strategies and technologies to overcome these challenges and ensure the effectiveness of drone operations in adverse weather conditions. Continued advancements in drone technology and ongoing research in this field will further enhance the capabilities of search and rescue missions, thereby improving disaster response and recovery efforts.

ACKNOWLEDGEMENTS

This research is funded by the Ministry of Higher Education (MOHE) Malaysia under the Trans-disciplinary Research Grant Scheme (TRGS) No: TRGS/1/2018/UITM/01/5/1 or 600-IRMI/TRGS 5/3 (001/2019), Universiti Teknologi MARA, Malaysia. We extend our gratitude to Aerodyne Group for their invaluable support in this research endeavor.





REFERENCES

- [1] S. Chowdhury, A. Emelogu, M. Marufuzzaman, S. G. Nurre, and L. Bian, "Drones for disaster response and relief operations: a continuous approximation model," *International Journal of Production Economics*, vol. 188, pp. 167–184, Jun. 2017, doi: 10.1016/j.ijpe.2017.03.024.
- [2] Y. Jahir, M. Atiquzzaman, H. Refai, A. Paranjothi, and P. G. LoPresti, "Routing protocols and architecture for disaster area network: a survey," *Ad Hoc Networks*, vol. 82, pp. 1–14, Jan. 2019, doi: 10.1016/j.adhoc.2018.08.005.
- [3] G. M. Dering, S. Micklethwaite, S. T. Thiele, S. A. Vollgger, and A. R. Cruden, "Review of drones, photogrammetry and emerging sensor technology for the study of dykes: best practises and future potential," *Journal of Volcanology and Geothermal Research*, vol. 373, pp. 148–166, Mar. 2019, doi: 10.1016/j.jvolgeores.2019.01.018.
- [4] D. R. A. Almeida *et al.*, "Monitoring the structure of forest restoration plantations with a drone-lidar system," *International Journal of Applied Earth Observation and Geoinformation*, vol. 79, pp. 192–198, Jul. 2019, doi: 10.1016/j.jag.2019.03.014.
- [5] O. Shrit, S. Martin, K. Alagha, and G. Pujolle, "A new approach to realize drone swarm using ad-hoc network," in *2017 16th Annual Mediterranean Ad Hoc Networking Workshop (Med-Hoc-Net)*, 2017, pp. 1–5, doi: 10.1109/MedHocNet.2017.8001645.
- [6] K. Mase, "Communication service continuity under a large-scale disaster: providing a wireless multihop network and shelter communication service for a disaster area under the Great East Japan Earthquake," in *2012 IEEE International Conference on Communications (ICC)*, Jun. 2012, pp. 6314–6318, doi: 10.1109/ICC.2012.6364749.
- [7] M. Avezum, A. Seitz, and B. Bruegge, "MODCAP: a platform for cooperative search and rescue missions," *AvioSE 2019: 1st Workshop on Avionics Systems and Software Engineering*, pp. 63–66, 2019.
- [8] S. Alani, Z. Zakaria, and H. Lago, "A new energy consumption technique for mobile ad hoc networks," *International Journal of Electrical and Computer Engineering (IJECE)*, vol. 9, no. 5, pp. 4147–4153, Oct. 2019, doi: 10.11591/ijece.v9i5.pp4147-4153.
- [9] N. Iqbal, M. S. Bin Abd Latiff, and S. M. Abdulhamid, "Energy aware routing protocol for energy constrained mobile ad-hoc





- networks,” *International Journal of Electrical and Computer Engineering (IJECE)*, vol. 8, no. 5, pp. 2979–2987, Oct. 2018, doi: 10.11591/ijece.v8i5.pp2979-2987.
- [10] K. W. Sung *et al.*, “PriMO-5G: making firefighting smarter with immersive videos through 5G,” in *2019 IEEE 2nd 5G World Forum (5GWF)*, Sep. 2019, pp. 280–285, doi: 10.1109/5GWF.2019.8911649.
- [11] S. Qazi, A. Alvi, A. M. Qureshi, B. A. Khawaja, and M. Mustaqim, “An architecture for real time monitoring aerial adhoc network,” in *2015 13th International Conference on Frontiers of Information Technology (FIT)*, Dec. 2015, pp. 154–159, doi: 10.1109/FIT.2015.36.
- [12] V.-P. Hoang, M.-H. Nguyen, T. Q. Do, D.-N. Le, and D. D. Bui, “A long range, energy efficient internet of things based drought monitoring system,” *International Journal of Electrical and Computer Engineering (IJECE)*, vol. 10, no. 2, pp. 1278–1287, Apr. 2020, doi: 10.11591/ijece.v10i2.pp1278-1287.
- [13] L. G. F. Kolobe, C. K. Lebekwe, and B. Sigweni, “Systematic literature survey: applications of LoRa communication,” *International Journal of Electrical and Computer Engineering (IJECE)*, vol. 10, no. 3, pp. 3176–3183, Jun. 2020, doi: 10.11591/ijece.v10i3.pp3176-3183.
- [14] L.-Y. Chen, H.-S. Huang, C.-J. Wu, Y.-T. Tsai, and Y.-S. Chang, “A LoRa-based air quality monitor on unmanned aerial vehicle for smart city,” in *2018 International Conference on System Science and Engineering (ICSSE)*, Jun. 2018, pp. 1–5, doi: 10.1109/ICSSE.2018.8519967.
- [15] A. Rahmadhani, Richard, R. Isswandhana, A. Giovani, and R. A. Syah, “LoRaWAN as secondary telemetry communication system for drone delivery,” in *2018 IEEE International Conference on Internet of Things and Intelligence System (IOTAIS)*, Nov. 2018, pp. 116–122, doi: 10.1109/IOTAIS.2018.8600892.
- [16] A. V. Leonov and G. A. Litvinov, “Simulation-based performance evaluation of AODV and OLSR routing protocols for monitoring and SAR operation scenarios in FANET with mini-UAVs,” *12th International Scientific and Technical Conference “Dynamics of Systems, Mechanisms and Machines”, Dynamics 2018*, 2018, doi: 10.1109/Dynamics.2018.8601494.
- [17] W. A. Hammood, S. M. @Asmara, R. A. Arshah, O. A. Hammood, H. Al Halbusi, and M. A. Al-Sharafi, “Factors influencing the success of information systems in flood early warning and response systems context,” *TELKOMNIKA (Telecommunication Computing Electronics and Control)*, vol. 18, no. 6, p. 2956, Dec. 2020, doi: 10.12928/telkomnika.v18i6.14666.
- [18] M. J. Abbas, H. M. Turki Alhilfi, and T. Sutikno, “Performance evaluation of two models in the reactive routing protocol in manets,” *Indonesian Journal of Electrical Engineering and Computer Science (IJECS)*, vol. 21, no. 1, pp. 391–397, 2021, doi: 10.11591/ijeecs.v21.i1.pp391-397.
- [19] G. M. Walunjkar and K. R. Anne, “Performance analysis of routing protocols in MANET,” *Indonesian Journal of Electrical Engineering and Computer Science (IJECS)*, vol. 17, no. 2, pp. 1047–1052, 2020, doi: 10.11591/IJECS.V17.I2.PP1047-1052.
- [20] H. Nawaz, H. M. Ali, and S. R. Massan, “A study of mobility models for UAV communication networks,” *3C Tecnología_Glosas de innovación aplicadas a la pyme*, no. 2, pp. 276–297, 2019, doi: 10.17993/3ctecno.2019.specialissue2.276-297.
- [21] O. S. Oubbati, M. Atiquzzaman, P. Lorenz, M. H. Tareque, and M. S. Hossain, “Routing in flying Ad Hoc networks: survey, constraints, and future challenge perspectives,” *IEEE Access*, vol. 7, no. June, pp. 81057–81105, 2019, doi: 10.1109/ACCESS.2019.2923840.
- [22] S. M. S. Mohd Daud *et al.*, “Applications of drone in disaster management: a scoping review,” *Science & Justice*, vol. 62, no. 1, pp. 30–42, Jan. 2022, doi: 10.1016/j.scijus.2021.11.002.
- [23] I. N. Azmi, Y. M. Yussoff, M. Kassim, and N. M. Tahir, “A mini-review of flying Ad Hoc networks mobility model for disaster areas,” *International Transaction Journal of Engineering*, vol. 12, no. 10, pp. 1–12, 2021, doi: 10.14456/ITJEMAST.2021.191.
- [24] M. S. Hakimiy Salem and F. H. Kamaru Zaman, “Effectiveness of human detection from aerial images taken from different heights,” *TEM Journal*, pp. 522–530, May 2021, doi: 10.18421/TEM102-06.
- [25] I. N. Azmi, Y. Mohd Yussoff, M. Kassim, and N. Md Tahir, “Coverage area of path planning mobility model for screening post-disaster area,” *Journal of Electrical & Electronic Systems Research*, vol. 19, no. OCT2021, pp. 74–79, Oct. 2021, doi: 10.24191/jeesr.v19i1.010.
- [26] Y. Chen, D. Baek, A. Bocca, A. Macii, E. Macii, and M. Poncino, “A case for a battery-aware model of drone energy consumption,” in *2018 IEEE International Telecommunications Energy Conference (INTELEC)*, Oct. 2018, vol. 2018-October, pp. 1–8, doi: 10.1109/INTLEEC.2018.8612333.
- [27] R. Shivgan and Z. Dong, “Energy-efficient drone coverage path planning using genetic algorithm,” in *2020 IEEE 21st International Conference on High Performance Switching and Routing (HPSR)*, May 2020, vol. 2020-May, pp. 1–6, doi: 10.1109/HPSR48589.2020.9098989.
- [28] M. Hwang, H.-R. Cha, and S. Y. Jung, “Practical endurance estimation for minimizing energy consumption of multirotor unmanned aerial vehicles,” *Energies*, vol. 11, no. 9, Art. no. 2221, Aug. 2018, doi: 10.3390/en11092221.
- [29] R. Battulwar *et al.*, “A practical methodology for generating high-resolution 3D models of open-pit slopes using UAVs: flight path planning and optimization,” *Remote Sensing*, vol. 12, no. 14, Jul. 2020, doi: 10.3390/rs12142283.
- [30] Y.-H. Tu, S. Phinn, K. Johansen, A. Robson, and D. Wu, “Optimising drone flight planning for measuring horticultural tree crop structure,” *ISPRS Journal of Photogrammetry and Remote Sensing*, vol. 160, pp. 83–96, Feb. 2020, doi: 10.1016/j.isprsjprs.2019.12.006.

BIOGRAPHIES OF AUTHORS







Intan Nabina Azmi     received a diploma and a B.Eng. (Hons) in electrical engineering (electronics) from Universiti Teknologi MARA (UiTM), Malaysia. In 2023, she earned her master’s degree in electrical engineering from UiTM Shah Alam, Malaysia. Currently, she pursues her PhD at the College of Engineering, UiTM Shah Alam, Malaysia. Her research interests are information delivery to wireless networks, mobile drone models, drone applications in disaster areas, nuclear reactor coolant system, machine learning, time series analysis. She can be contacted at email: hellointan.azmi@gmail.com.







Murizah Kassim     is a Senior Research Fellow at Institute for Big Data Analytics and Artificial Intelligence (IBDAAI). She is also an associate professor from the School of Electrical Engineering, College of Engineering, UiTM, Shah Alam, Selangor. She received her PhD in engineering from Universiti Kebangsaan Malaysia (UKM). Her research areas are computer network, data engineering, IoT, web and mobile development applications. She is also an associate member of Enabling Internet of Things Technologies (EIIoTT) RIG UiTM and a member of MBOT, IEEE, IET, IAENG and IACSIT. She can be contacted at email: murizah@uitm.edu.my.



Yusnani Mohd Yusoff     is Head of Information, Security and Trusted Infrastructure Laboratory or InSTIL Research Interest Group (RIG). She is also an associate professor at the College of Engineering, UiTM, Shah Alam Malaysia. Her research area focusses on trusted authentication, embedded security and secure internet of thing focusing on the smart home and smart cities devices. She is also a member of internet of things working group under the Malaysia Technical Standard Forum Bhd and a member of IEEE, IAENG and Board of Engineer Malaysia. She can be contacted at email: yusna233@uitm.edu.my.



Nooritawati Md Tahir     is a professor at the College of Engineering, Universiti Teknologi MARA (UiTM), Malaysia. Her research interest is in the field of image processing, pattern recognition and computational intelligence. She received her PhD in electrical engineering from Universiti Kebangsaan Malaysia (UKM), master's in engineering from University of Liverpool UK and degree in electronics engineering from Institut Teknologi MARA (ITM). She is also a Chartered Engineer (CEng) registered with the Engineering Council UK and senior member of IEEE. She can be contacted at: nooritawati@ieee.org.